Proceedings of IMECE2005
2005 ASME International Mechanical Engineering Congress and Exposition
November 5-11, 2005, Orlando, Florida, USA

IMECE2005-80873

ULTRAFAST LASER RADIATION AND CONDUCTION HEAT TRANSFER IN BIOLOGICAL TISSUES

Kyunghan Kim
Dept. of Mechanical and Aerospace Engineering
Rutgers, The State University of New Jersey
Piscataway, NJ 08854, USA
khkim74@eden.rutgers.edu

Zhixiong Guo
Dept. of Mechanical and Aerospace Engineering
Rutgers, The State University of New Jersey
Piscataway, NJ 08854, USA
Corresponding author: guo@jove.rutgers.edu

ABSTRACT

Ultrafast laser radiation heat transfer in biological tissues is governed by time-dependent equation of radiative transfer and modeled using the transient discrete ordinates method. The divergence of radiative heat flux is then obtained and used for predicting the local temperature response due to radiation energy absorption within the ultrashort time period. To this end, the lumped method is employed and heat diffusion is negligible. Both single pulse and pulse train irradiations are considered. For the single pulse irradiation, the transient radiation field is obtained and the local temperature keeps rising until a time of about 20 times of the short pulse width; and then a stable local temperature profile is reached and maintained until the start of heat conduction. For the pulse train case (10^4 ultrashort pulses until 1 ms), the local temperature response is an accumulation of continuous single pulses because the thermal relaxation time of biological tissues was reported in the range of 1-100 sec and is much longer than the pulse train duration (1 ms). After a stable local temperature field is achieved, the hyperbolic heat conduction model is adopted to describe the heat conduction. MacCormark's scheme is utilized for solving the thermal wave equations. Thermal wave behavior is observed during the heat transfer process. It is found that the hyperbolic wave model predicts a higher temperature rise than the classical heat diffusion model. After several thermal relaxation times the thermal wave behavior is substantially weakened and the predictions between the hyperbolic and diffusion models match.

INTRODUCTION

The study of short-pulsed laser radiation transport in biological tissues is attracting increasingly attention in recent years. Ultrafast radiation transfer is usually accompanied with the use of ultrashort-pulsed lasers. Ultrafast lasers with pulse width in the range from sub-nanoseconds down to femtoseconds can be used in a wide spectrum of emerging biomedical technologies such as in optical tomography [1,2], laser tissue ablation [3], laser surgery [4], and photodynamic therapy [5], to name a few. Laser is also the excitation source in fluorescence imaging, scanning and labeling [6]. Fundamental to these applications is ultrafast laser radiation transport and associated heat transfer in biological tissues.

Due to the very short time duration in the radiation-matter interaction and transport processes, traditional radiation transfer model and Fourier's heat conduction model may not be valid for describing ultrafast laser radiation and conduction heat transfer. For example, our previous studies [7, 8] have shown that the propagation of radiation with the speed of light brings many unique features in ultrafast radiation transfer and the neglect of the time-derivative term in the equation of radiation transfer (ERT), that is valid in traditional radiation heat transfer, will lead to erroneous results. The concept of ultrafast radiation transfer [9] was introduced in order to differentiate it from conventional transient radiation transfer in that only the time-dependence of boundary conditions is considered, but the ERT is still stationary. In ultrafast radiation transfer, both the governing equation and boundary conditions are time-dependent and radiation propagates with the speed of light. We have found that, when the pulse width of an incident laser is less than or comparable to the order of the characteristic time scale for radiation propagation defined by $t_c = L_c / c$ (L_c is the characteristic length), ultrafast radiation transfer should be incorporated.

Numerical methods for solving the transient ERT have been extensively reported in the literature [7-14]. Among them, the transient discrete ordinates method (TDOM) has been applied to two-dimensional [12] and three-dimensional [13] rectangular coordinate systems and curvilinear geometric problems [14]. It was found that the TDOM could give

 Copyright © 2005 by ASME

satisfactory results for modeling ultrafast laser radiation heat transfer in turbid media.

Heat conduction is always associated with laser radiation absorption in biological tissues. The study of heat transfer is of particular interest in laser treatment and safety. For example, prediction of thermal response is a critical issue in laser tissue welding and soldering. Laser welding of tissue is a surgical technique for bonding of tissues by using a laser beam to activate photothermal bonds and/or photochemical bonds. This method is potentially more advantageous than the conventional suturing technique because it is a non-contact method, which does not introduce foreign materials, and it is capable of forming an immediate watertight seal. For over 30 years, laser tissue welding has been extensively studied [4] as an alternative tool for tissue closure. In order to achieve optimum welding strength, a proper temperature at the welding region was reported at 62.2 ± 2°C [15]. Pulsed lasers were applied to reduce the collateral thermal damage [16, 17]. Thus, it is needed to properly model heat transfer during ultrafast laser radiation transport in biological tissues which is a coupled radiative-conductive heat transfer problem.

For irradiation times less than 10 sec, the heat transfer can be modeled as a heat conduction problem; and the influence of blood perfusion only plays a minor role and is negligible [18]. Fourier heat conduction equation (parabolic type) implies an infinite speed of thermal propagation and is traditionally used for describing heat diffusion. For a physical process occurring in a time interval shorter than that required for attaining thermal equilibrium, however, it has been noticed that heat wave theory must be adopted [19-21]. The thermal wave postulate leads to hyperbolic heat conduction equations and suggests a finite speed of thermal propagation. Mitra et al. [22] and Tzou [23] provided some experimental evidences of hyperbolic heat conduction. Thermodynamic validity of the hyperbolic equations and the range of parameters where non-Fourier considerations are significant have also been examined [24, 25]. Glass et al. [26] approached the hyperbolic conduction problems numerically using MacCormack's scheme. Some other numerical methods [27-30] have also been recently considered.

Vedavarz et al. [25] have analyzed the relaxation time of thermal wave for various materials. They found that the thermal relaxation time of biological tissues was in the range of 1-100 sec at room temperature, which are several orders of magnitude larger than that of metallic and semiconductor materials. Kaminski [20] estimated the thermal relaxation time between 20 and 30 sec for meat products. Mitra et al. [22] measured a 16 sec thermal relaxation time for processed meat. Such larger relaxation times in biological tissues make the hyperbolic heat conduction specifically significant in the thermal modeling of laser-tissue interactions.

The objective of this work is to analyze the radiation transport and thermal response in tissues subjected to irradiation of ultrashort laser pulses. In the present study, the ultrafast radiation heat transfer in tissues is governed by the time-dependent equation of radiation transfer (ERT) and solved using the TDOM method. The hyperbolic heat conduction equations are solved using the finite difference method based on MacCormark's scheme. Since the speed of thermal wave in biological tissues is over 10 orders of magnitude smaller than that of light. Thus, the coupling of radiative-conductive heat transfer involves two different time scales. The heat transfer in ultrafast laser-tissue interaction is a multi-scale and multi-physics problem. In order to examine the non-Fourier effects, the transient thermal responses obtained from the hyperbolic heat conduction modeling are also compared with those obtained from the classical parabolic heat diffusion equation.

NOMENCLATURE

c	= speed of light
C_p	= specific heat
c_t	= speed of thermal wave
D	= spot width of laser sheet
G	= incident radiation
h	= heat transfer coefficient
I	= radiation intensity
L	= length
n	= number of angular discretization
Q	= non-dimensional heat flux
q	= heat flux
S	= source term
T	= temperature
t	= time
t_p	= pulse width
W	= width
x,y	= coordinates
Greek symbols	
α	= thermal diffusivity
χ, η	= non-dimensional coordinates
δ	= penetration depth
μ^l, η^l, ξ^l	= directional cosines
w	= angular weight
θ	= non-dimensional temperature
ρ	= density
σ_a	= absorption coefficient
σ_e	= extinction coefficient
σ_s	= scattering coefficient
τ	= thermal relaxation time
ω	= scattering albedo
ξ	= non-dimensional time
Subscripts	
b	= blackbody
$cond$	= conduction
i	= initial
i,j	= indices of grid
ref	= reference
rad	= radiation
Superscripts	
l	= discrete direction index
n	= time level

MATHEMATICAL MODELS

Governing Equations

Copyright © 2005 by ASME

The speed of thermal wave c_t is defined as

$$c_t = \sqrt{\alpha/\tau}\ , \tag{1}$$

where α is the thermal diffusivity and τ is the thermal relaxation time. The reported thermal diffusivity of tissues is in the range of 0.1 – 0.2 mm^2/s [31, 32]. In the present calculations, we suppose $\alpha = 0.12$ mm^2/s and $\tau = 15$ s; then $c_t = 0.09$ mm/sec.

Radiation is transported in the speed of light, i.e. c = 0.2 mm/ps in biological tissues. It is about 12 orders of magnitude faster than the speed of thermal wave. Thus, during the time scale of ultrashort pulse or pulse train (up to the order of 1 ms) the transport of thermal wave and heat diffusion are negligible.

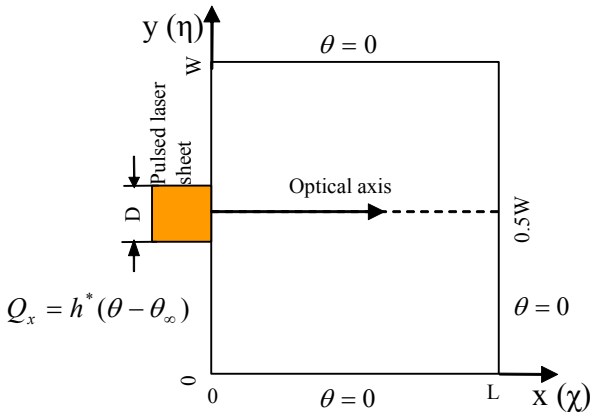

Fig.1. Schematic diagram of the simulation model.

Consider a collimated laser pulse incidence upon a 2-D biological tissue as shown in Fig. 1. The local temperature response of the tissue to an ultrashort pulse can be simply expressed as

$$\rho C_p \frac{\partial T(x,y,t)}{\partial t} = \nabla \cdot q_{rad}(x,y,t)\,, \tag{2}$$

where ρ is the density, C_p is the specific heat, and $\nabla \cdot q_{rad}(x,y,t)$ is the divergence of radiative heat flux due to radiation absorption that is calculated by

$$\nabla \cdot q_{rad}(x,y,t) = \sigma_a (4\pi I_b - G)\,, \tag{3}$$

where σ_a is the absorption coefficient of the tissue and I_b is the black body emissive power which is negligible because the tissue can be treated as a cold medium as compared to the large flux of laser beam. The incident radiation, G, is a direction-integrated radiation intensity and can be obtained by the summation of angle-discretized radiation intensity.

To calculate the radiative intensity I^l in a discrete ordinate, time-dependent ERT in discrete-ordinate format is introduced:

$$\frac{1}{c}\frac{\partial I^l}{\partial t} + \xi^l \frac{\partial I^l}{\partial x} + \eta^l \frac{\partial I^l}{\partial y} + \sigma_e I^l = \sigma_e S^l, l = 1,2,3,\ldots,n \tag{4}$$

where ξ^l and η^l are the directional cosine in a discrete ordinate direction, σ_e is the extinction coefficient that is the sum of the absorption and scattering coefficients, and S^l is the radiative source term from the laser radiation.
that can be expressed as

$$S^l = (1-\omega) I_b + \frac{\omega}{4\pi} \sum_{i=1}^{n} w^j \Phi^{il} I^i + S_c^l, \quad l = 1,2,..,n, \tag{5}$$

Here, the scattering albedo is $\omega = \sigma_s/\sigma_e$ and the scattering phase function is $\Phi\ (\hat{s}^i \to \hat{s}^l)$. A quadrature set of n discrete ordinate with the appropriate angular weight w^l $(l = 1,2,..,n)$ is used. The laser source S_c^l in Eq. (5) is the driving force of the transient radiation heat transport and can be expressed as

$$S_c^l = \frac{\omega}{4\pi} I_c (\mu^c \mu^l + \eta^c \eta^l + \xi^c \xi^l), \tag{6}$$

where the unit vector of (μ^c, η^c, ξ^c) represents the collimated laser incident direction.

After the ultrashort pulse effect is diminished in a very short time period, the temperature response reaches to a pseudo steady state; and then thermal wave transport starts. To predict the transient temperature field during thermal wave transport, the hyperbolic heat conduction equations are introduced [19]:

$$\tau \frac{\partial q_{cond,x}(x,t)}{\partial t} + q_{cond,x}(x,t) = -k \frac{\partial T(x,y,t)}{\partial x}, \tag{7-1}$$

$$\tau \frac{\partial q_{cond,y}(y,t)}{\partial t} + q_{cond,y}(y,t) = -k \frac{\partial T(x,y,t)}{\partial y}. \tag{7-2}$$

where k is the thermal conductivity, T and q represent temperature and heat flux, respectively.

The energy equation is expressed as

$$\rho C_p \frac{\partial T(x,y,t)}{\partial t} = -\left(\frac{\partial q_{cond,x}(x,t)}{\partial x} + \frac{\partial q_{cond,y}(y,t)}{\partial y} \right). \tag{8}$$

For the sake of analysis, the hyperbolic conduction equations and energy equation are converted to non-dimensional forms as follows:

$$\frac{\partial Q_\chi}{\partial \xi} + \frac{\partial \theta}{\partial \chi} + 10 Q_\chi = 0\,, \tag{9-1}$$

$$\frac{\partial Q_\eta}{\partial \xi} + \frac{\partial \theta}{\partial \eta} + 10 Q_\eta = 0\,, \tag{9-2}$$

$$\frac{\partial \theta}{\partial \xi} + \frac{\partial Q_\chi}{\partial \chi} + \frac{\partial Q_\eta}{\partial \eta} = 0\,, \tag{9-3}$$

where non-dimensional variables are defined by

$$Q_\chi = \frac{q_{cond,x}\sqrt{\alpha\tau}}{k(T_{ref} - T_i)}, \; Q_\eta = \frac{q_{cond,y}\sqrt{\alpha\tau}}{k(T_{ref} - T_i)}, \; \theta = \frac{T - T_i}{T_{ref} - T_i},$$

$$\chi = \frac{x}{10\sqrt{\alpha\tau}}, \; \eta = \frac{y}{10\sqrt{\alpha\tau}}, \; \xi = \frac{t}{10\tau}. \tag{10}$$

Copyright © 2005 by ASME

In which, T_i and T_{ref} are the cold tissue and reference temperatures, respectively.

Boundary Conditions

For radiation heat transfer, reflection and refraction governed by Snell's law and Fresnel equation, respectively, are considered at the tissue/are interface. At the rest boundaries, diffuse reflections are considered. For details, please refer to our recent publications [12-14].

The incident laser sheet has a Gaussian profile both temporally and spatially and can be expressed by

$$I_c(x,y,t) = I_{c0}\exp\left\{-4\ln 2\times[(t-x/c)/t_p-1.5]^2\right\} \times\exp[-(y-W/2)^2/\nu^2]\times\exp(-\sigma_e x) \quad (11)$$

in which I_{c0} is the peak amplitude of the intensity which is set as 5×10^{-6} in the present calculations, t_p is the pulse width, and ν is the spatial variance factor. The Gaussian spatial ratio ν/D is chosen as 1.0, where D is the width of the laser sheet. The reference temperature is calculated from the incident laser pulse by

$$T_{ref} = T_i + \frac{\int_0^{3t_p} N_p\sigma_a I_c(x=0,y=W/2,t)dt}{\rho C_p}. \quad (12)$$

where, N_p is the number of the laser pulses.

For hyperbolic heat conduction, the boundary conductions are specified below.

$$\theta(\chi,\eta,\xi)=0 \text{ , for } \eta=0 \text{ or } \eta=\eta_{\max}=W/(10\sqrt{\alpha\tau}) \quad (13\text{-}1)$$

$$\theta(\chi,\eta,\xi)=0 \text{ , for } \chi=\chi_{\max}=L/(10\sqrt{\alpha\tau}) \quad (13\text{-}2)$$

$$Q_x = h^*(\theta-\theta_\infty) \text{ , for } \chi=0 \quad (13\text{-}3)$$

where θ_∞ is the non-dimensional ambient temperature and $h^*=\sqrt{\alpha\tau}h/k$ with h as the heat transfer coefficient.

The following lists several assumptions we adopted when set up the present model:

(1) Thermal radiation emission at the tissue/air interface is negligible because the surface temperature is low such that the blackbody intensity is much smaller than the incident laser intensity.

(2) The tissue optical and thermal properties are thermally stable during the heat transfer processes.

(3) Thermal evaporation and phase change (from solid to soft) of tissue are not considered.

(4) The heating of tissue is treated by the lumped method for bulk material. The abrupt electron temperature rise during ultrashort time period is neglected.

Numerical Schemes

To solve the time-dependent ERT, the TDOM is employed. The tissue geometry is divided into a uniform grid of 200×200. The solid angle is divided by a quadrature set of $n=N(N+2)$ discrete ordinates for S_N method. In the present study, we use the S_{10} scheme. The time step selected is 0.2 ps. Details of the numerical schemes have been described in our recent publications [12-14]; thus, they are not repeated here.

To solve the hyperbolic heat conduction equations, MacCormack's predictor-corrector scheme is adopted. The hyperbolic equations include the discontinuities in front of thermal waves. MacCormack's predictor-corrector scheme has been known to deal with wave propagation very well in a 1-D hyperbolic heat conduction problem [26]. Thus, it is extended to the 2-D problem in the present study. The discretized forms of these equations are as follows:

Predictor:

$$\tilde{Q}^{n+1}_{x\,i,j} = (1-10\Delta\xi)\,Q^n_{x\,i,j} - \frac{\Delta\xi}{\Delta\chi}\left(\theta^n_{i+1,j}-\theta^n_{i,j}\right), \quad (14\text{-}1)$$

$$\tilde{Q}^{n+1}_{\eta\,i,j} = (1-10\Delta\xi)\,Q^n_{\eta\,i,j} - \frac{\Delta\xi}{\Delta\eta}\left(\theta^n_{i,j+1}-\theta^n_{i,j}\right), \quad (14\text{-}2)$$

$$\tilde{\theta}^{n+1}_{i,j} = \theta^n_{i,j} - \frac{\Delta\xi}{\Delta\chi}\left(Q^n_{\chi i+1,j}-Q^n_{\chi i,j}\right) - \frac{\Delta\xi}{\Delta\eta}\left(Q^n_{\eta i,j+1}-Q^n_{\eta i,j}\right), \quad (14\text{-}3)$$

Corrector:

$$Q^{n+1}_{x\,i,j} = \frac{1}{2}\left[Q^n_{x\,i,j} + \tilde{Q}^{n+1}_{x\,i,j} - \frac{\Delta\xi}{\Delta\chi}\left(\tilde{\theta}^{n+1}_{i,j}-\tilde{\theta}^{n+1}_{i-1,j}\right) - 10\Delta\xi\,\tilde{Q}^{n+1}_{x\,i,j}\right], \quad (14\text{-}4)$$

$$Q^{n+1}_{\eta\,i,j} = \frac{1}{2}\left[Q^n_{\eta\,i,j} + \tilde{Q}^{n+1}_{\eta\,i,j} - \frac{\Delta\xi}{\Delta\eta}\left(\tilde{\theta}^{n+1}_{i,j}-\tilde{\theta}^{n+1}_{i,j-1}\right) - 10\Delta\xi\,\tilde{Q}^{n+1}_{\eta\,i,j}\right], \quad (14\text{-}5)$$

$$\theta^{n+1}_{i,j} = \frac{1}{2}[\theta^n_{i,j} + \tilde{\theta}^{n+1}_{i,j} - \frac{\Delta\xi}{\Delta\chi}(\tilde{Q}^{n+1}_{\chi\,i,j} - \tilde{Q}^{n+1}_{\chi\,i-1,j}) - \frac{\Delta\xi}{\Delta\eta}(\tilde{Q}^{n+1}_{\eta\,i,j} - \tilde{Q}^{n+1}_{\eta\,i,j-1})]. \quad (14\text{-}6)$$

To solve these finite difference equations, the same grid system as the radiative transfer problem is chosen. The non-dimensional time step for the thermal wave problem is selected as the same as the grid size, i.e., $\Delta\xi=\Delta\chi=\Delta\eta$, such that a unity Courant number is used.

RESULTS AND DISCUSSION

The sketch of the tissue geometry is shown in Fig. 1. For simplicity, we considered a square tissue (L = W = 13.416 mm) such that $\chi_{\max}=\eta_{\max}=1$. The optical and thermal properties are chosen as porcine cartilage tissue [33]: σ_a = 0.1 mm^{-1}, σ_s = 2.6 mm^{-1} (reduced scattering coefficient), α = 0.12 mm^2/s, $T_i = 310$ K, and $\rho C_p = 5.04\times10^6$ J/(m$^3\cdot$K). The ultrashort laser pulse width is 10 ps and the width of incident laser sheet is 2.6832 mm. The heat transfer coefficient h is 15 W/(m^{2}K).

Figure 2 shows the profiles of the divergence of radiative heat flux for a single pulse irradiation along the optical axis direction at several selected time instants. A steep gradient of the divergence of radiative heat flux is found for early time

Copyright © 2005 by ASME

instant (t = 20 ps). As time advancing, the profiles become flat and the magnitude of overall strength decreases. At t = 500 ps, the profile shows a quite symmetric shape against the central point at $\chi = 0.5$ and its magnitude drops to the order of 10^{-13}. This implies that the radiation absorption of this pulse has almost been completed by this time stage.

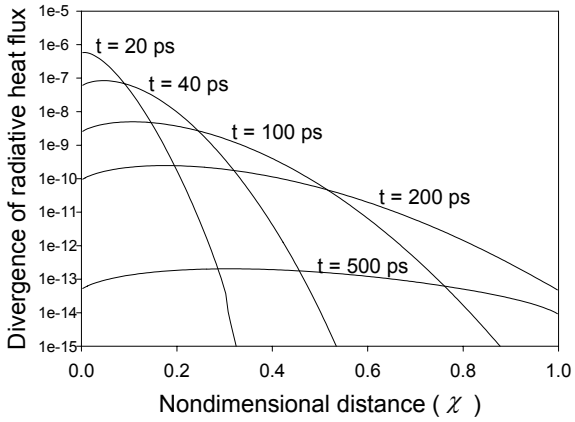

Fig. 2. The profiles of divergence of radiative heat flux along the optical axis with several selected time instants.

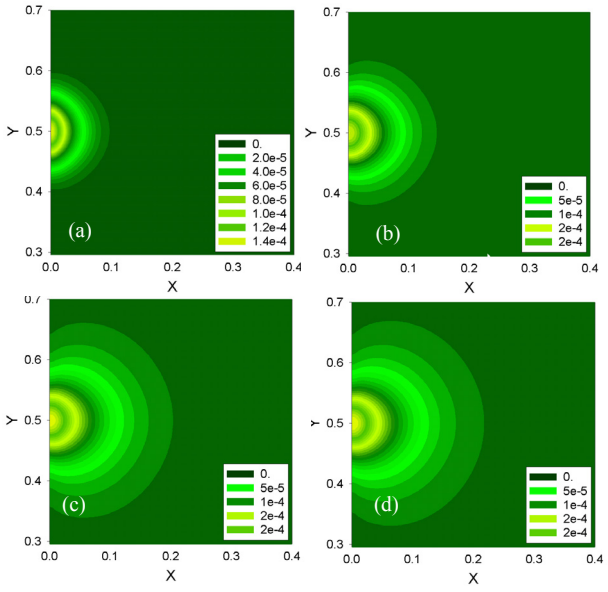

Fig. 3 The contours of temperature distribution for a single pulse irradiation at selected time instants: (a) t = 20 ps, (b) t = 40 ps, (c) t = 100 ps, and (d) t = 200ps.

Figure 3 shows the contours of the local temperature distribution at three time instants. At early time stage (t = 20 ps), the temperature field is concentrated on the laser deposition area but the magnitude of it is small. As time proceeds, the temperature field is propagating to the surrounding tissue due to radiation transport and the temperature reaches to a high level due to the accumulation of radiation absorption. Around t = 200 ps, the local temperature field reaches to a pseudo steady state and maintained until the start of heat conduction.

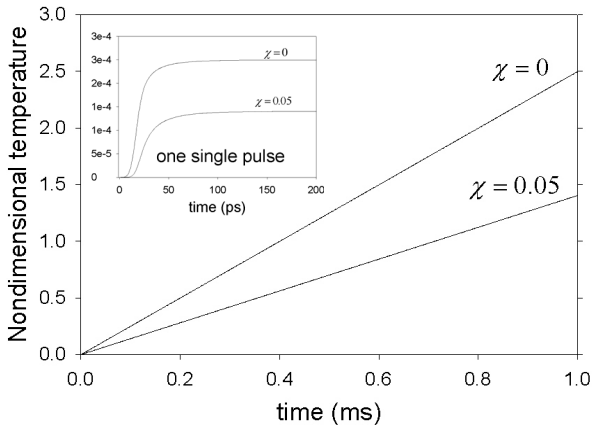

Fig. 4. The temporal profiles of temperature for a single pulse and pulse train at two optical axis positions.

The pulse train effect is investigated in Figure 4. The pulse train consists of 10^4 short pulses (t_p = 10 ps) uniformly generated within 1 ms. After 1 ms, the laser is turned off. Since the pulse train duration is much shorter than the thermal relaxation time of the tissue (τ is assumed to be 15 sec), no heat diffusion and thermal wave should be considered. The local temperature response is an accumulation of continuous single pulses.

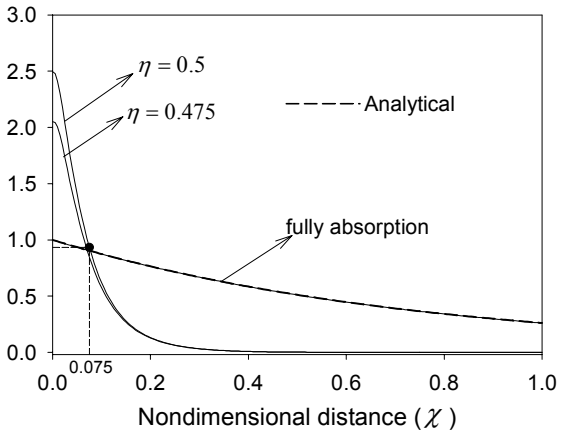

Fig. 5. The spatial variance of temperature profiles at 1 ms for two selected lines: $\eta = 0.5$ and $\eta = 0.475$; and comparison of temperature profiles between numerical and analytical solutions for a purely absorbing medium with absorption coefficient $\sigma_a = 0.1$ mm^{-1}.

Figure 5 shows the spatial variance of the non-dimensional temperature profiles in the tissue at time of 1 ms. We also

Copyright © 2005 by ASME

compare the numerical result with the analytical solution for the case of purely absorption tissue (σ_a = 0.1 mm^{-1}). It is seen that both analytical and numerical results match very well. As we know, thermal relaxation time can be calculated by a definition [31]:

$$\tau_r = \frac{\delta^2}{4\alpha} \tag{15}$$

where δ is the penetration depth. For the fully absorbing medium, δ is generally treated as $1/\sigma_a$; and then $\tau_r \approx 208$ sec. For the absorbing and scattering tissue, if we consider δ is the depth measured to 37% of the maximum temperature rise along the optical axis, then $\delta/\left(10\sqrt{\alpha\tau}\right)$ equals to 0.075. And the calculated thermal relaxation time is $\tau_r \approx 0.1406, \tau = 2.1$ sec.

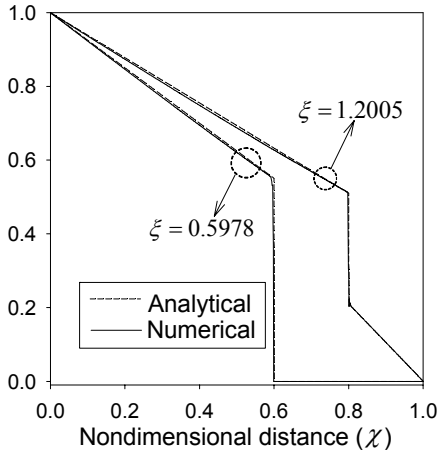

Fig. 6. Comparison between the numerical and exact solutions for an exemplary 1-D slab problem.

Following the arrival of a pseudo stable local temperature field the thermal wave propagation starts and the temperature field is governed by the hyperbolic heat conduction equations. To validate the code for hyperbolic conduction simulation, a comparison between the present numerical simulation and a published analytical solution [26] for hyperbolic conduction in a 1-D slab is shown in Fig. 6. It is seen that the present calculations match the counterparts of analytical solution very well.

Now, the numerical simulation is extended to the 2-D case. The temperature profiles along three selected cross lines are exhibited in Figs. 7 (a), (b) and (c), respectively. Several time instants are selected for comparison. The wave behavior of temperature propagation is very obvious in the figures. The local temperature profiles at initial stage due to radiation absorption in the ultrashort time period show a perfect Gaussian distribution. Starting from $\xi = 0.05$ in Fig. 7 (a), the evolution of thermal waves takes place. The profiles are symmetric against the center. The amplitude of temperature wave gradually decreases as time marches. As the wave propagates from the center position to the tissue edge, the wave peak becomes small. At long time stage, the wave behavior retards and gradually disappears. Then the diffusion process starts. Similar wave behavior is shown in Fig. 7 (b) and (c) as well. However, the onset time of wave evolution is delayed to $\xi = 0.1$ in Fig. 7 (b) and to $\xi = 0.2$ in Fig. 7 (c).

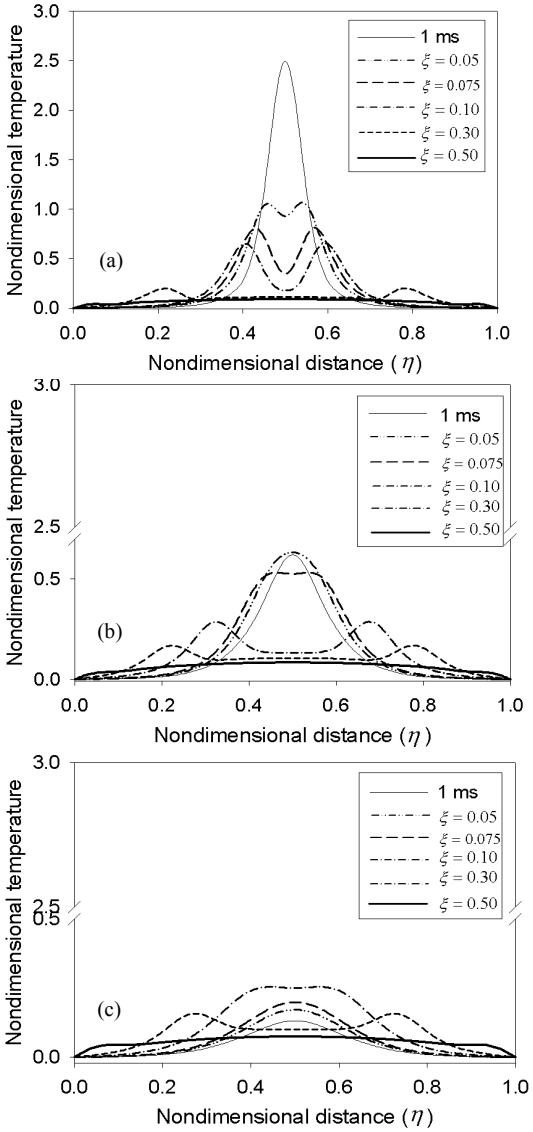

Fig. 7. The time history of temperature profiles along three selected cross lines: (a) $\chi = 0$, (b) $\chi = 0.1$, and (c) $\chi = 0.2$.

The hyperbolic temperature field in the tissue and its time history are depicted in Fig. 8. At early time instants the temperature response is confined in a small area close to the laser spot. As time increases, the thermal influencing zone (higher temperature than surrounding area) enlarges with clear wave evolution inside the zone. At long time stage ($\xi = 0.5$), a diffusion field is forming in the whole tissue model.

Copyright © 2005 by ASME

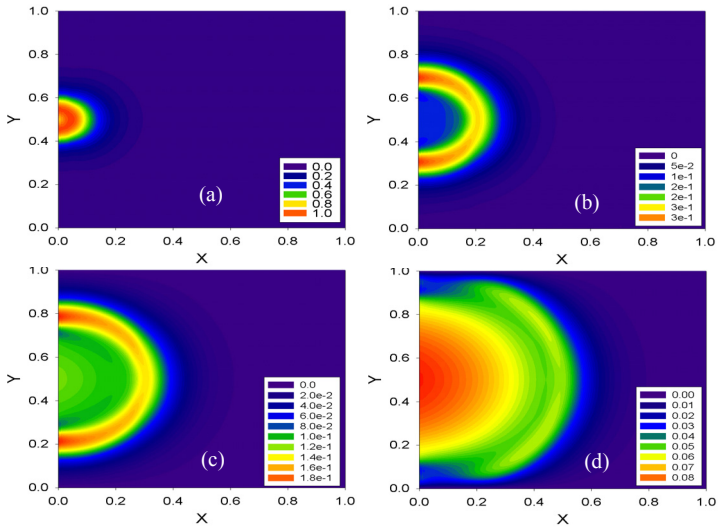

Fig. 8. The contours of hyperbolic conduction temperature field at several selected time instants: (a) $\xi = 0.05$, (b) $\xi = 0.2$, (c) $\xi = 0.3$, and (d) $\xi = 0.5$.

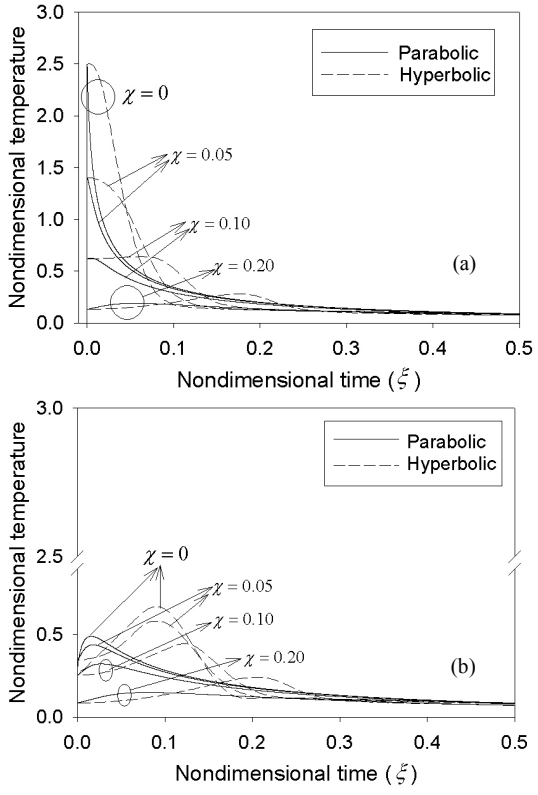

Fig. 9. Comparison of temporal profiles of temperature between hyperbolic conduction and parabolic conduction models: (a) $\eta = 0.5$ and (b) $\eta = 0.4$.

To understand well the hyperbolic effects, the temperature profiles predicted by the hyperbolic model and Fourier parabolic model, respectively, are compared in Fig. 9, where the comparisons of the temporal variance of temperature profiles at different locations are presented. In hyperbolic conduction modeling, wave behavior exists and the temperature changes periodically with a decreasing amplitude. In parabolic conduction modeling, the temperature decays exponentially and more slowly than the hyperbolic prediction. Also the predicted maximum temperature values by the hyperbolic model are much larger than those by the parabolic model. In order to prevent the overheating in laser tissue interactions, an appropriate hyperbolic heat transfer model must be adopted. At long time, the thermal behavior disappears and the predictions between the hyperbolic and parabolic models are consistent.

CONCLUSIONS

A combined hyperbolic radiation and conduction heat transfer model was developed to simulate the multi-scale and multi-physics heat transfer problem in ultrafast laser radiation and tissue interactions. Subject to the incidence of an ultrashort laser pulse or pulse train, the local temperature inside the tissue was found to rise very fast and this rise was purely because of local radiation absorption resulting from transient radiation heat transport. During a short time period, the local temperature field reached to a pseudo steady state until the start of thermal wave propagation. The thermal wave phenomenon can be well described by the hyperbolic heat conduction equations. The wave behavior was observed from the contours of the 2-D temperature field as well as the temperature profiles along the optical axis and cross lines. The evolution of thermal wave took place earlier near the laser beam spot. As time increases, the thermal influencing zone enlarges with clear wave evolution inside the zone. The difference between the hyperbolic modeling and parabolic modeling was obvious. In the hyperbolic conduction modeling, wave behavior exists and the temperature changes periodically with a decreasing amplitude. In the parabolic conduction modeling, however, the temperature decays exponentially and more slowly than the hyperbolic prediction. Also the predicted maximum temperature values by the hyperbolic model are much larger than those by the parabolic model. After about five thermal relaxation times, the difference between the diffusion modeling and hyperbolic modeling is slight.

ACKNOWLEDGMENTS

Z. Guo acknowledges the partial support of this research via an Industrial University Research Award (NJSGC 03-44) from the New Jersey Space Grant Consortium and the Metropolitan Technologies Consulting Group, LLC.

REFERENCES

1. M.S. Patterson, B. Chance and B. C. Wilson, "Time-resolved reflectance and transmittance for the non-invasive

Copyright © 2005 by ASME

measurement of tissue optical properties," *Appl. Opt*., 28, 2331-2336 (1989).
2. R. R. Alfano, S. G. Demos and S. K. Gayen, "Advances in optical imaging of biomedical media," *Ann. New York Acad. Sci.*, 820, 248-270 (1997).
3. F.H Loesel, F.P Fisher, H. Suhan, and J. F Bille, "Non-thermal ablation of neural tissue with fetmtosecond laser pulses," *Appl. Phys. B.,* 66, 121-128 (1998).
4. L.S. Bass and M.R. Treat, "Laser tissue welding: a comprehensive review of current and future applications," *Lasers Surg. Med*., 17, 315-349 (1995).
5. A. Obana and Y. Gohto, "Scanning laser system for photodynamic therapy of choroidal neovascularization", *Lasers Surgery Med*., 30, 370-375 (2002).
6. H. Quan and Z. Guo, "Fast 3-D optical imaging with transient fluorescence signals," *Optics Express*, 12, 449-457 (2004).
7. Z. Guo and S. Kumar, "Radiation element method for transient hyperbolic radiative transfer in plane-parallel inhomogeneous media," *Numerical Heat Transfer Part B: Fundamentals*, 39, 371 – 387 (2001).
8. Z. Guo, J. Aber, B. Garetz and S. Kumar, "Monte Carlo simulation and experiments of pulsed radiative transfer," *J. Quantitative Spectroscopy & Radiative Transfer*, 73, 159 – 168 (2002).
9. Z. Guo and K.H. Kim, "Ultrafast-laser-radiation transfer in heterogeneous tissues with the discrete-ordinates method," *Appl. Opt.*, 42, 2897-2905 (2003).
10. S. Kumar, K. Mitra and Y. Yamada, "Hyperbolic damped-wave models for transient light-pulse propagation in scattering media", *Appl. Opt*., 35, 3372-3378 (1996).
11. K. Mitra and S. Kumar, "Development and comparison of models for light pulse transport through scattering absorbing media", *Appl. Opt*., 38, 88-196 (1999).
12. Z. Guo and S. Kumar, "Discrete ordinates solution of short pulse laser transport in two-dimensional turbid media," *Appl. Opt.*, 40, 3156-3163 (2001).
13. Z. Guo and S. Kumar, "Three-dimensional discrete ordinates method in transient radiative transfer," *J. Thermophy. Heat Transfer*, 16, 289-296 (2002).
14. K.H. Kim and Z. Guo, "Ultrafast radiation heat transfer in laser tissue welding and soldering," *Numerical Heat Transfer Part A: Applications*, 46, 23-46 (2004).
15. G.M. Leola, R.R. Anderson, S. Decocted, "Preliminary evaluation of collagen as a component in the thermally induced weld," *Proc SPIE*, 1422, 116-122 (1991).
16. L.L. Deckelbaum, J.M. Isner, R.F. Donaldson, S.M. Laliberte, R.H. Clarke, D.N. Salem, "Use of pulsed energy delivery to minimize tissue injury resulting from CO_2 laser irradiation of cardiovascular tissues", *J. Am Coll Cardiol,* 7, 898-900 (1986).
17. R.R. Anderson, and J.A. Parrish., "Selective photothermolysis: precise microsurgery by selective absorption of pulsed radiation", *Science*, 220, 525-527 (1983).
18. A.J. Welch, E.H. Wissler and L.A. Priebe, "Significance of blood flow in calculation of temperature in laser irradiated tissue," *IEEE Trans. Biomed. Eng.*, BME-27, 164-166 (1980).
19. D.D. Joseph and L. Preziosi, "Heat waves", *Rev. Modern Phys.*, 61, 118-1128 (1989).
20. W. Kaminski, "Hyperbolic heat conduction equation for materials with a nonhomogeneous inner structures," *J. Heat Transfer*, 112, 555-560 (1990).
21. M.N. Ozisik and D.Y. Tzou, "On the wave theory in heat conduction," *J. Heat Transfer*, 116, 526-535 (1994).
22. K. Mitra, S. Kumar, A. Vedavarz, and M. Moallemi, "Experimental evidence of hyperbolic heat conduction in processed meat," *J. Heat Transfer*, 117, 568-573 (1995)
23. D. Y. Tzou, "Experimental support for the lagging behavior in heat propagation," *J. Thermophys. heat transfer,* 9, 686-693 (1995).
24. A.S. Lavine and C. Bai, "Hyperbolic heat conduction in thin domains," *Thermal Sci. & Eng.*, 2, 185-190 (1994).
25. A. Vedavarz, S. Kumar and M.K. Moallemi, "Significance of non-Fourier heat waves in conduction," *J. Heat transfer,* 116, 221-224 (1994).
26. D.E. Glass, M.N. Ozisik, D.S. McRae, B. Vick, "On the numerical solution of hyperbolic heat conduction," *Numerical Heat Transfer*, 8, 497-504 (1985).
27. A. Saidane and S. H. Pulko, "High-power short pulse laser heating of low dimensional structures: a hyperbolic heat conduction study using TLM," *Microelectronic Engineering,* 51-52, 469-478 (2000).
28. L. H. Liu and H.P. Tan, "Non-Fourier effects on transient coupled radiative-conductive heat transfer in one-dimensional semitransparent medium subjected to a periodic irradiation," *J. Quantitative Spectroscopy & Rad. Transfer*, 71, 11-24 (2001).
29. Q.M, Fan and W.Q. Lu, "A new numerical method to simulate the non-Fourier heat conduction in a single-phase medium," *Int. J. Heat Mass Transf.*, 45, 2815-2821 (2002).
30. E. Hoashi, T. Yokomine, A. Shimizu and T. Kunugi, "Numerical analysis of wave-type heat transfer propagating in a thin foil irradiated by short-pulsed laser," *Int. J. Heat Mass Transfer*, 46, 4083-4095 (2003).
31. B. Choi and A.J. Welch, "Analysis of thermal relaxation during laser irradiation of tissue", *Lasers in Surg Med.,* 29, 351-359 (2001).
32. S.A. Telenkov, J.I. Youn, D.M. Goodman, A.J. Welch and T.E. Milner, "Non-contact measurement of thermal diffusivity in tissue," *Phys. Med. Biol*., 46, 551-558 (2001).
33. S.H. Diaz, G. Aguilar, R. Basu, E. Lavernia, and B.J.F. Wong, "Modeling the thermal response of porcine cartilage to laser irradiation," *Proc SPIE*, 4617, 47-56 (2002).

Copyright © 2005 by ASME